Influence of Wall Properties on the Peristaltic Flow of a Nanofluid in View of the Exact Solutions: Comparisons with Homotopy Analysis Method

Abdelhalim Ebaid and Salem H. Alatawi

Department of Mathematics, Faculty of Science, University of Tabuk, P. O. Box 741, Tabuk 71491, Saudi Arabia

Reprint requests to A. E.; E-mail: aebaid@ut.edu.sa

Z. Naturforsch. **69a**, 199 – 206 (2014) / DOI: 10.5560/ZNA.2014-0010

Received November 11, 2013 / revised January 27, 2014 / published online April 16, 2014

No doubt, the exact solution of any physical system is considered optimal when it is available. Such exact solution is of great importance not only in validating the accuracy of the approximate solution obtained for the same problem but also to derive the correct physical interpretation of the involved physical phenomena. In this paper, the system of linear and nonlinear partial differential equations describing the peristaltic flow of a nanofluid in a channel with compliant walls has been solved exactly. These exact solutions have been implemented to explore the exact effects of Prandtl number Pr, thermophoresis parameter N_{T}, Brownian motion parameter N_{B}, and Eckert number Ec on the temperature, the nanoparticle concentration profiles, and the heat transfer coefficient $Z(x)$. In addition, the exact results have been compared with a very recent work via the homotopy analysis method for the same problem. Although these comparisons showed that the published approximate results coincide with the current exact analysis, a few remarkable differences have been detected for the behaviour of the heat transfer coefficient.

Key words: Peristaltic Flow; Wall Properties; Nanofluid; Exact Solution; Homotopy Analysis Method.

1. Introduction

During the past decades, the subject of peristaltic flow of classical newtonian and non-newtonian fluids have been discussed by many authors [1 – 30] for its important applications in medicine and biology. For examples, peristaltic flow occurs widely in the functioning of the ureter, chyme movement in the intestine, movement of eggs in the fallopian tube, the transport of the spermatozoa in cervical canal, transport of bile in the bile duct, transport of cilia, circulation of blood in small blood vessels, and the transport of intra-uterine fluid within the cavity of the uterus. For application in biology, Mekheimer and Abd elmaboud [25] showed that the peristaltic flow of blood with bio-heat transfer is of great importance in destroying undesirable tissues, such as cancer. It was also clarified in [31] that in the case of hyperthermia, the tissue can be destroyed when heated to 42 – 45 °C.

However, very little efforts are devoted to examining peristaltic flow of nanofluids. Nano-scale particle added fluids are called as nanofluid. Normally, if the particle sizes are in the 1 – 100 nm ranges, they are generally called nano-particles, 1 nm (nano-meter) $= 10^{-9}$ m. The term nanofluid may be first used by Choi [32] to describe a fluid in which nanometer-sized particles are suspended in conventional heat transfer basic fluids. Fluids such as oil, water and ethylene glycol mixture are poor heat transfer fluids, since the thermal conductivity of these fluids play important role on the heat transfer coefficient between the heat transfer medium and the heat transfer surface. Numerous methods have been taken to improve the thermal conductivity of these fluids by suspending nano/micro or larger-sized particle materials in liquids. An innovative technique to improve heat transfer is by using nano-scale particles in the base fluid [32]. Choi et al. [33] showed that the addition of a small amount (less than 1% by volume) of nanoparticles to conventional heat transfer liquids increased the thermal conductivity of the fluid up to approximately two times. This phenomenon suggests the possibility of using

nanofluids in advanced nuclear systems (Buongiorno and Hu [34]).

Although thousands of papers are available for the peristaltic transport of classical fluids, a few studies were presented for peristaltic flow of nanofluids [35 – 39] since the first investigation of Akbar and Nadeem [35]. In [35], the authors discussed the endoscopic effects on the peristaltic flow of a nanofluid in a uniform tube. One year after, Akbar et al. [36] have analyzed the peristaltic flow of a nanofluid in a non-uniform tube. Moreover, Akbar and Nadeem [37] investigated the peristaltic flow of a Phan-Thien–Tanner nanofluid in a diverging tube. In addition, the influence of wall properties on the peristaltic flow of a nanofluid has been discussed very recently by Mustafa et al. [38]. Besides, the effect of the slip conditions on the peristaltic flow of a nanofluid in an asymmetric channel has been also analyzed by Akbar et al. [39] and Ebaid and Aly [40]. The main notice here is about the approximate solution method that has been used by the authors in [35], [36], and [39]. In these just mentioned studies, the authors used the homotopy perturbation method (HPM) to obtain the analytical approximate solutions for the governing system. However, their approximate solutions did not give the correct behaviour of the physical quantities as clarified very recently by Ebaid and Aly [40]. For more illustrations, Ebaid and Aly [40] re-investigated the problem of Akbar and Nadeem [35]. They have obtained the exact solutions of the system of linear and nonlinear partial differential equations describing the flow. These exact solutions have been used to show that the physical discussion provided by Akbar and Nadeem [35] for the temperature distribution and the nanoparticle concentration were incorrect when compared with those exactly obtained by Ebaid and Aly [40]. In [41 – 43], some other useful works on nanofluid flow are listed.

Of course, the exact solution of any physical system is not always available, however, when it is obtained we can highly trust with the physical interpretation derived from such exact solution. Due to the detected remarkable differences between the approximate results obtained by the series solution method (HPM) and those exactly provided in [40], we may conclude that much effort should be first spent for searching for the exact solution before attacking the problem via any of the approximate series solution. In addition, if it is impossible to obtain the exact solution of the considered problem, we can instead use any of the approximate solution methods [44 – 50] and in this case the issue of convergence should be addressed to ensure the accuracy. Accordingly, we aim in this paper to report new exact analytical results for the influence of the wall properties on the peristaltic flow of a nanofluid [38]. Therefore, this problem will be re-investigated in the current paper and our objectives can be summarized as follows:

- The first task is to obtain the exact solutions for the system of partial differential equations governing the flow.
- The obtained exact solutions shall be used to introduce various plots for the exact curves of the temperature distribution, the nanoparticle concentration, and the heat transfer coefficient.
- The final task is to check whether there are differences between the approximate results reported in [38] by using the homotopy analysis method (HAM) and those exactly obtained in the current paper.

2. The Physical Problem

Mustafa et al. [38] considered the peristaltic flow of an incompressible nanofluid in a channel of uniform thickness. The axial and the transverse directions are denoted by x and y. They have found that under the assumptions of long wavelength and low Reynolds number approximation the flow is governed by the following system of partial differential equations in non-dimensional form [38]:

$$\frac{\partial^4 \psi}{\partial y^4} = 0\,, \tag{1}$$

$$\frac{1}{\mathrm{Pr}}\frac{\partial^2 \theta}{\partial y^2} + N_{\mathrm{B}}\frac{\partial \theta}{\partial y}\frac{\partial \phi}{\partial y} + N_{\mathrm{T}}\left(\frac{\partial \theta}{\partial y}\right)^2 + \mathrm{Ec}\left(\frac{\partial^2 \psi}{\partial y^2}\right)^2 = 0\,, \tag{2}$$

$$\frac{\partial^2 \phi}{\partial y^2} + \frac{N_{\mathrm{T}}}{N_{\mathrm{B}}}\frac{\partial^2 \theta}{\partial y^2} = 0\,, \tag{3}$$

where Pr, N_{T}, N_{B}, and Ec are respectively Prandtl number, the thermophoresis parameter, the Brownian motion parameter, and Eckert number. The flow was subjected to the boundary conditions

$$\begin{aligned}
&\frac{\partial \psi}{\partial y} = 0 \ \text{ at } \ y = \pm\eta\,,\\
&\frac{\partial^3 \psi}{\partial y^3} = \left[E_1 \frac{\partial^3}{\partial x^3} + E_2 \frac{\partial^3}{\partial x \partial t^2} + E_3 \frac{\partial^2}{\partial t \partial x}\right]\eta\\
&\qquad \text{at } \ y = \pm\eta\,,\\
&\theta = 0\,, \ \ \phi = 0 \ \text{ at } \ y = -\eta\,,\\
&\theta = 1\,, \ \ \phi = 1 \ \text{ at } \ y = +\eta\,,\\
&\qquad \eta = 1 + \varepsilon \sin[2\pi(x-t)]\,.
\end{aligned} \tag{4}$$

The system (1)–(4) has been approximately solved in [38] by using the homotopy analysis method. The approximate series solution obtained in [38] was used to discuss various physical phenomena such as temperature profile, nanoparticle concentration, and the heat transfer coefficient. However, the exact solutions of the above system can be obtained and this is the subject of the next section.

3. The Exact Solutions

It is observed from (3) that it can be easily integrated w. r. t. y to give

$$\frac{\partial \phi}{\partial y} = -\left(\frac{N_\mathrm{T}}{N_\mathrm{B}}\right)\frac{\partial \theta}{\partial y} + f_1(x)\,, \tag{5}$$

where $f_1(x)$ is an unknown function. Further integration of (5) w. r. t y leads to the following exact relation between the temperature and the nanoparticle concentration:

$$\phi(x,y) = -\left(\frac{N_\mathrm{T}}{N_\mathrm{B}}\right)\theta(x,y) + f_1(x)y + f_2(x)\,, \tag{6}$$

where $f_2(x)$ is a further unknown function. On applying the boundary conditions in (4), we have

$$\begin{aligned}
f_1(x) &= \frac{1}{2\eta}\left(1 + \frac{N_\mathrm{T}}{N_\mathrm{B}}\right),\\
f_2(x) &= \frac{1}{2}\left(1 + \frac{N_\mathrm{T}}{N_\mathrm{B}}\right).
\end{aligned} \tag{7}$$

Therefore, we obtain $\phi(x,y)$ in terms of $\theta(x,y)$ in the following exact form:

$$\phi(x,y) = \frac{1}{2}\left(1 + \frac{N_\mathrm{T}}{N_\mathrm{B}}\right)\left(1 + \frac{y}{\eta}\right) - \left(\frac{N_\mathrm{T}}{N_\mathrm{B}}\right)\theta(x,y)\,. \tag{8}$$

On substituting (5) into (2) yields a partial differential equation in only θ:

$$\frac{\partial^2 \theta}{\partial y^2} + \left[N_\mathrm{B}\mathrm{Pr} f_1(x)\right]\frac{\partial \theta}{\partial y} = -\mathrm{PrEc}\left(\frac{\partial^2 \psi}{\partial y^2}\right)^2, \tag{9}$$

which can be solved exactly to give

$$\begin{aligned}
\theta(x,y) = \theta(x,0) &- \frac{1}{N_\mathrm{B}\mathrm{Pr} f_1(x)}\left[\mathrm{e}^{-N_\mathrm{B}\mathrm{Pr} f_1(x) y} - 1\right]\\
&\cdot \theta_y(x,0) - \mathrm{PrEc}\, I(y)\,,
\end{aligned} \tag{10}$$

where $I(y)$ is given as

$$\begin{aligned}
I(y) = \int_0^y \mathrm{e}^{-N_\mathrm{B}\mathrm{Pr} f_1(x)\mu} \int_0^\mu \mathrm{e}^{N_\mathrm{B}\mathrm{Pr} f_1(x)\sigma}\\
\cdot \left[\left(\frac{\partial^2 \psi}{\partial y^2}\right)^2\right]_{y=\sigma} \mathrm{d}\sigma\, \mathrm{d}\mu\,.
\end{aligned} \tag{11}$$

Applying the boundary conditions on θ as given in (4), we obtain

$$\begin{aligned}
\theta(x,0) &= \mathrm{PrEc} I(-\eta) + \frac{1}{2}\left[\mathrm{e}^{N_\mathrm{B}\mathrm{Pr} f_1(x)\eta} - 1\right]\\
&\quad \cdot \mathrm{csch}\big(N_\mathrm{B}\mathrm{Pr} f_1(x)\eta\big)\\
&\quad \cdot \Big[1 - \mathrm{PrEc}\big(I(-\eta) - I(\eta)\big)\Big]\,,\\
\theta_y(x,0) &= \frac{1}{2} N_\mathrm{B}\mathrm{Pr} f_1(x)\Big[1 - \mathrm{PrEc}\big(I(-\eta) - I(\eta)\big)\Big]\\
&\quad \cdot \mathrm{csch}\big(N_\mathrm{b}\mathrm{Pr} f_1(x)\eta\big)\,.
\end{aligned} \tag{12}$$

Therefore

$$\begin{aligned}
\theta(x,y) = \mathrm{PrEc}\big[I(-\eta) - I(y)\big] &+ \frac{1}{2}\big[1 - \mathrm{PrEc}(I(-\eta)\\
&- I(\eta))\big] \cdot \left[\mathrm{e}^{N_\mathrm{B}\mathrm{Pr} f_1(x)\eta} - \mathrm{e}^{-N_\mathrm{B}\mathrm{Pr} f_1(x) y}\right]\\
&\cdot \mathrm{csch}\big(N_\mathrm{B}\mathrm{Pr} f_1(x)\eta\big)\,.
\end{aligned} \tag{13}$$

Here, it should be noted that the exact analytical solutions for the temperature distribution θ and the concentration function ϕ are expressed in terms of the integration $I(y)$. However, $I(y)$ which is defined by (11) depends on the stream function ψ. The exact solution of this stream function has been already obtained by Mustafa et al. [38] and is given as

$$\psi = \Omega(x,t)\left(y^3 - 3\eta^2 y\right), \tag{14}$$

where

$$\begin{aligned}
\Omega(x,t) = \frac{4\pi^3\varepsilon}{3}\Bigg[&\frac{E_3}{2\pi}\sin 2\pi(x-t)\\
&- (E_1 + E_2)\cos 2\pi(x-t)\Bigg]\,.
\end{aligned} \tag{15}$$

The substitution of (14) into (11) leads to the following explicit form for $I(y)$:

$$I(y) = \frac{12\Omega^2(x,t)}{(N_{\mathrm{B}}\mathrm{Pr}f_1(x))^4}\Big[6\Big(\mathrm{e}^{-N_{\mathrm{B}}\mathrm{Pr}f_1(x)y} - 1\Big) + 6\big(N_{\mathrm{B}}\mathrm{Pr}f_1(x)y\big) - 3\big(N_{\mathrm{B}}\mathrm{Pr}f_1(x)y\big)^2 + \big(N_{\mathrm{B}}\mathrm{Pr}f_1(x)y\big)^3\Big]. \tag{16}$$

4. Numerical Results

In the previous section, the exact solutions for the temperature and the nanoparticle concentration have been obtained. Really, such exact solutions are of great importance and certainly would lead to a better understanding of the physical aspects of the model. Here, the obtained exact solutions are used to explore the actual effects of various parameters on the temperature distribution, the nanoparticle concentration, and the coefficient of heat transfer. In Figures 1 – 5, we have chosen $t = 0.1$, $x = 0.2$, $\varepsilon = 0.2$, $E_1 = 0.01$, $E_2 = 0.02$, and $E_3 = 0.01$. Figure 1a depicts the effect of Brownian motion parameter N_{B} on the temperature profiles at $N_{\mathrm{T}} = 0.1$, $\mathrm{Pr} = \mathrm{Ec} = 1.0$. Figure 1b indicates the effects of the thermophoresis parameter N_{T} on the

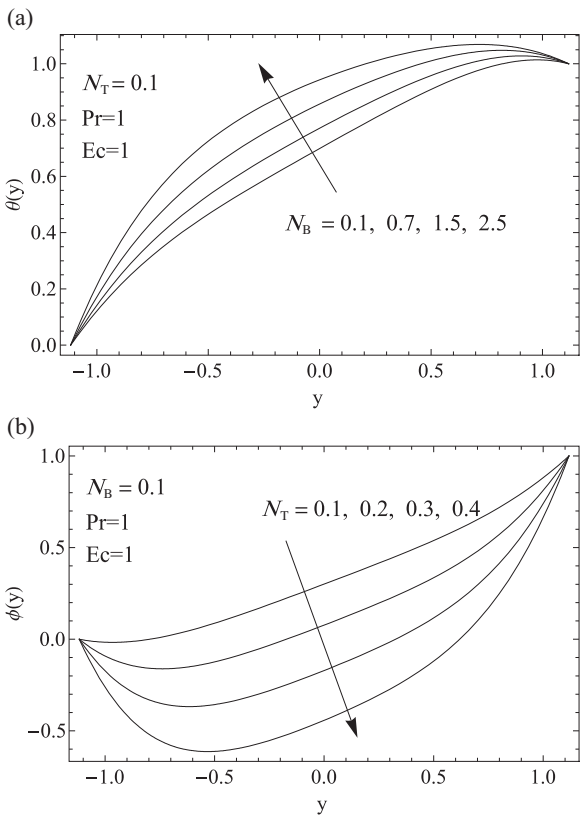

Fig. 1. (a) Exact influence of N_{B} on the temperature distribution. (b) Exact influence of N_{T} on the concentration.

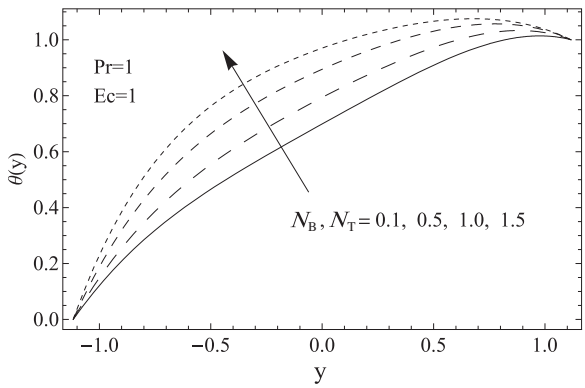

Fig. 2. Exact influence of N_{B} and N_{T} on the temperature distribution.

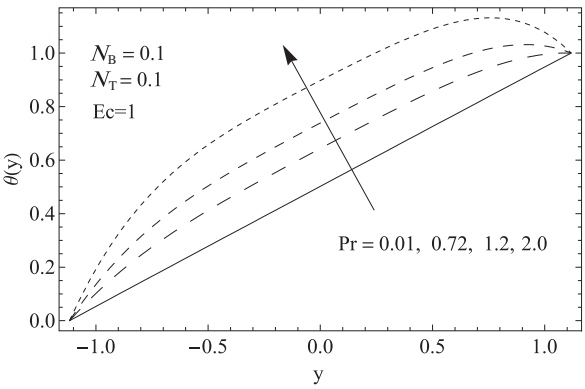

Fig. 3. Exact influence of Pr on the temperature distribution.

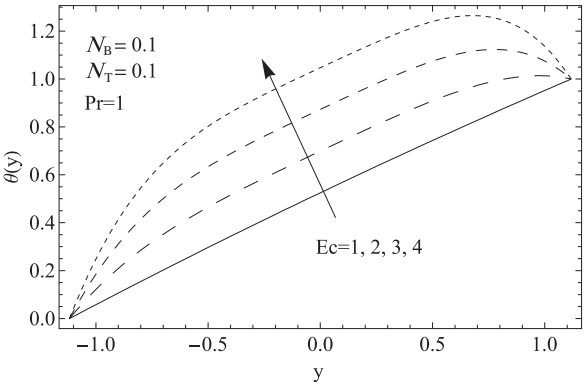

Fig. 4. Exact influence of Ec on the temperature distribution.

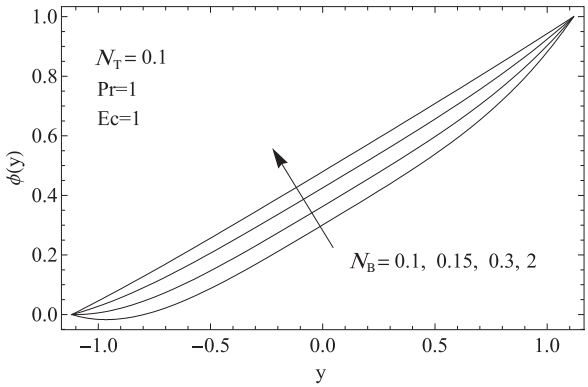

Fig. 5. Exact influence of N_B on the nanoparticle concentration.

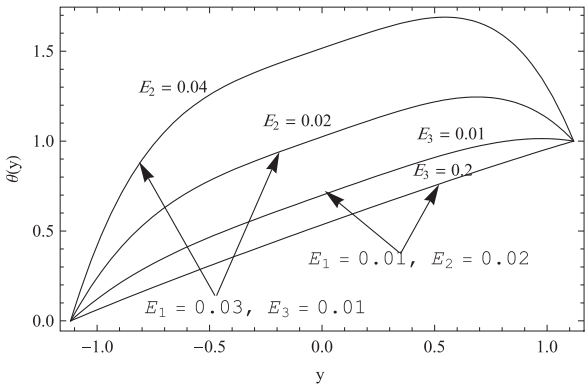

Fig. 6. Exact influence of E_1, E_2, and E_3 on the temperature distribution.

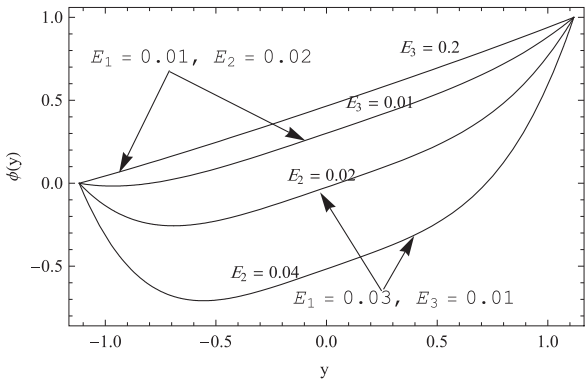

Fig. 7. Exact influence of E_1, E_2, and E_3 on the nanoparticle concentration.

nanoparticle concentration at $N_B = 0.1$, $\mathrm{Pr} = \mathrm{Ec} = 1.0$. The results displayed in Figures 1a and 1b agree with the corresponding results in Figures 2a and 2b in [38] which have been obtained by both the numerical solution (using NDSolve command in MATHEMATICA 8) and the series solution using the homotopy analysis method.

The exact influence of Brownian motion and thermophoresis parameters on the temperature θ is shown in Figure 2. It can be seen from Figure 2 of the current paper and Figure 3 in [38] that the approximate numerical results in [38] are very close to the present exact results. As commented by Mustafa et al. [38], it is observed from Figure 2 that there is a substantial increase in the temperature with an increase in N_B and N_T. As the Brownian motion and thermophoretic effects strengthen this corresponds to the effective movement of the nanoparticles from the wall to the fluid which results in the significant increase in the temperature θ. Figures 3 and 4 depict the exact effects of Prandtl number Pr and Eckert number Ec on the temperature θ. It is also observed from these figures that the current exact results coincide with those approximately obtained via the homotopy analysis method by

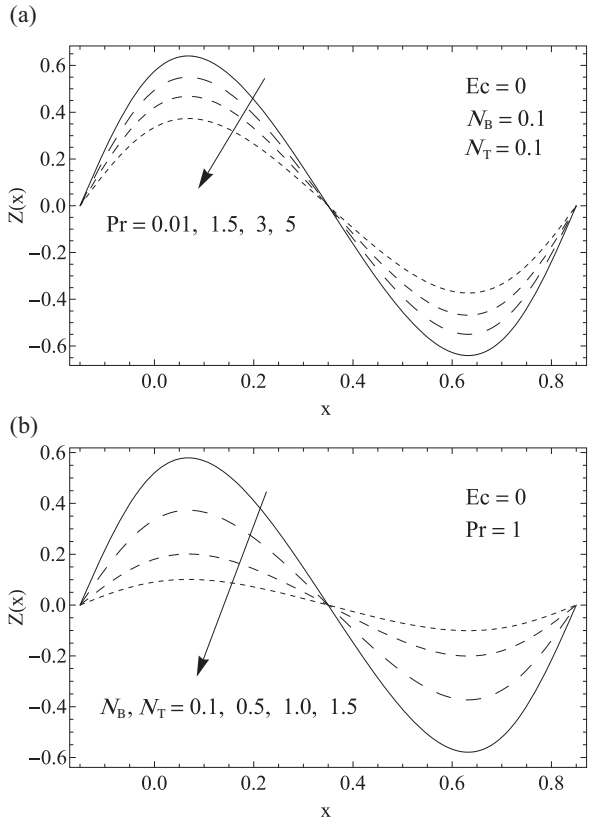

Fig. 8. (a) Influence of Pr on $Z(x)$ when $\mathrm{Ec} = 0$. (b) Influence of N_B and N_T on $Z(x)$ when $\mathrm{Ec} = 0$.

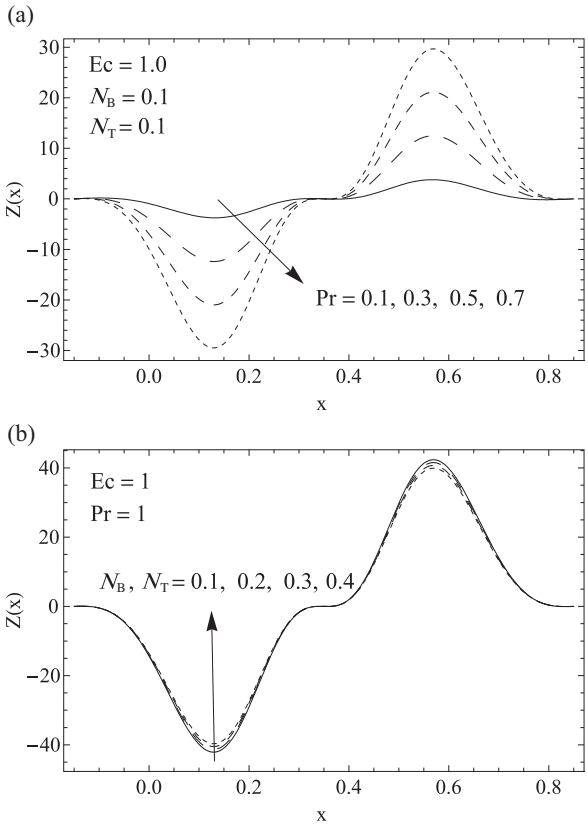

Fig. 9. (a) Influence of Pr on $Z(x)$ when Ec = 1. (b) Influence of N_B and N_T on $Z(x)$ when Ec = 1.

Figures 4 and 5 in [38], where the physical description of these figures has been also introduced.

Regarding the effects of N_B on the nanoparticles concentration ϕ, Figure 5 shows the exact variation of ϕ against y at the same values of the physical parameters taken by Mustafa et al. [38]. Figure 5 indicates that the nanoparticles concentration increases (it was mentioned decreases in [38]) as the Brownian motion effect intensifies [38]. As pointed out in [38], it is interesting to see that the smaller values of N_B strongly affect the concentration function ϕ. However the nanoparticles concentration is negligibly affected for values of N_B beyond 2. For more illustration of this point, we can easily see from Figure 5 that ϕ behaves as a straight line against y when $N_B = 2$. This certain behaviour of the concentration function ϕ occurs for any values of $N_B \geq 2$. Our exact results in Figure 6 declares that the temperature increases with an increase in E_2 while it decreases with an increase in E_3. Such behaviour for the temperature is identical to the results depicted in Figure 7 by the authors [38]. Figure 7 shows that the exact nanoparticles concentration ϕ is a decreasing function in E_2. In this case, the results given by [38] in Figure 8 need revision, where it was mentioned that ϕ is an increasing function in E_2. However, Figure 7 of the current paper shows that there is a slight decrease in the nanoparticles concentration when there is an increase in E_3 and this agrees with the conclusion made about the upper two curves in Figure 8 given by [38].

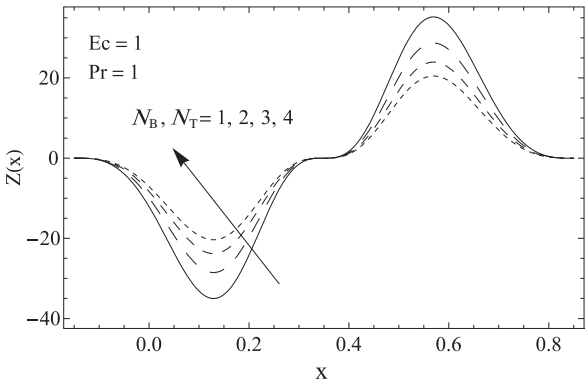

Fig. 10. Influence of large values of N_B and N_T on $Z(x)$ when Ec = 1.

Figures 8 and 9 show the impacts of various parameters on the heat transfer coefficient. In these figures, the same data considered in [38] have been selected, where $t = 0.1$, $\varepsilon = 0.2$, $E_1 = 0.1$, $E_2 = 0.1$, and $E_3 = 0.01$. The coefficient of heat transfer at the wall is defined by $Z(x) = \eta_x \theta_y(\eta)$, where it gives the rate of heat transfer (or equivalently heat flux) at the upper wall. It can be seen from Figures 8a and 8b that when the viscous dissipation effect vanishes, i. e., (Ec = 0), the heat flux $Z(x)$ has an oscillatory behaviour which is expected in view of peristalsis. Figures 8a and 8b show that the absolute value of the heat transfer coefficient decreases upon increasing the values of N_B, N_T, and Pr. The current exact numerical results obtained in Figures 8a and 8b are in full agreement with those approximately obtained by Mustafa et al. [38] in Figures 9a and 9b. Similar to the observations noted by Mustafa et al. [38], the absolute value of the heat transfer coefficient increases with an increase in Pr when the viscous dissipation effect is significantly large (Ec = 1) as shown in Figure 9a. However, a remarkable difference is found between the current exact range in which $Z(x)$ varies and the approximate one obtained by Figure 10a in [38]. In addition, great remarkable differences have been detected between the current numerical results

(Fig. 9b) and those obtained in [38] (Fig. 10b) regarding the effects of N_B and N_T on the heat transfer coefficient. Our exact results presented in Figure 9b reveal that the absolute value of heat transfer coefficient decreases upon increasing the values of N_B and N_T. However, the situation was completely different in Figure 10b [38]. In order to confirm our point of view, additional plots are presented in Figure 10 to show that the absolute value of heat transfer coefficient decreases upon increasing the values of N_B and N_T.

5. Conclusion

In this paper, the system of partial differential equations describing the influence of wall properties on peristaltic flow of a nanofluid has been solved exactly. The obtained exact solutions have been used to study the effects of the Prandtl number Pr, thermophoresis parameter N_T, the Brownian motion parameter N_B, and Eckert number Ec on the temperature, the nanoparticle concentration profiles, and the heat transfer coefficient $Z(x)$. The obtained exact results have been compared with approximate analytical results obtained very recently via the homotopy analysis method in [38]. Although these comparisons clarified the high accuracy of the approximate results obtained in [38], little remarkable differences have been detected for the behaviour of the heat transfer coefficient. These accurate numerical results [38] comes back to the convergence control of the homotopy analysis method if compared with the incorrect results derived from the homotopy perturbation method [35] in which the convergence issue was not addressed. A final note on the current comparative study is that when it is difficult to achieve the exact solutions of the considered physical problem, we instead search for the approximate solutions by using any of the series method in which the convergence issue must be addressed.

[1] T. W. Latham, Fluid motion in a peristaltic pump, M. Sc. Thesis, MIT, Cambridge, MA, 1966.
[2] A. H. Shapiro, M. Y. Jaffrin, and S. L. Weinberg, J. Fluid Mech. **37**, 799 (1969).
[3] T. F. Zien and S. A. Ostrach, J. Biomech. **3**, 63 (1970).
[4] J. S. Lee and Y. C. Fung, Microvasc. Res. **3**, 272 (1971).
[5] S. E. Charm and G. S. Kurland, Blood flow and microcirculation, John Wiley, New York 1974.
[6] T. D. Brown, T. K. Hung, J. Fluid Mech. **83**, 249 (1977).
[7] D. A. Drew, Phys. Fluids **22**, 2081 (1979).
[8] S. Takabatake and K. Ayukawa, J. Fluid Mech. **122**, 439 (1982).
[9] L. M. Srivastava, V. P. Srivastava, and S. N. Sinha, Biorheol. **20**, 153 (1983).
[10] S. Takabatake, K. Ayukawa, and A. Mori, J. Fluid Mech. **193**, 267 (1988).
[11] L. M. Srivastava and V. P. Srivastava, Rheol. Acta **27**, 428 (1988).
[12] P. B. Cotton and C. B. Williams, Practical Gastrointestinal Endoscopy, Oxford University Press, Third edition, London 1990.
[13] D. Tang and M. Shen, J. Math. Anal. Appl. **174**, 265 (1993).
[14] E. F. El Shehawey and Kh. S. Mekheimer, J. Phys. D: Appl. Phys. **27**, 1163 (1994).
[15] J. C. Misra and S. K. Pandey, Comput. Math. Appl. **28**, 131 (1994).
[16] B. V. Rathish Kumar and K. B. Naidu, Comput. Fluids **24**, 161 (1995).
[17] R. A. Ramachandra and S. Usha, J. Fluid Mech. **298**, 271 (1995).
[18] J. C. Misra and S. K. Pandey, Math. Comput. Model. **22**, 137 (1995).
[19] V. P. Srivastava and L. M. Srivastava, Int. J. Eng. Sci. **35**, 1359 (1997).
[20] O. Eytan, A. J. Jaffa, and D. Elad, Med. Eng. Phys. **23**, 473 (2001).
[21] K. S. Mekheimer, Biorheol. **39**, 755 (2002).
[22] K. Vajravelu, S. Sreenadh, and V. R. Babu, Int. J. Nonlin. Mech. **40**, 83 (2005).
[23] K. S. Mekheimer and Y. Abd elmaboud, Appl. Math. Inform. Sci. **2**, 103 (2008).
[24] K. S. Mekheimer, Phys. Lett. A **372**, 4271 (2008).
[25] K. S. Mekheimer and Y. Abd elmaboud, Phys. Lett. A **372**, 1657 (2008).
[26] Kh. S. Mekheimer and Y. Abd elmaboud, Physica A **387**, 2403 (2008).
[27] S. Akram and S. Nadeem, Int. J. Numer. Methods Fluids **70**, 1475 (2012).
[28] N. Sher Akbar, S. Nadeem, and M. Ali, Heat Transf. Res. **43**, 69 (2012).
[29] N. Sher Akbar and S. Nadeem, Int. J. Heat Mass Transf. **55**, 3964 (2012).
[30] R. Ellahi, A. Riaz, S. Nadeem, and M. Ali, Math. Probl. Eng. **2012**, (2012), Article ID 329639, 24 pages.
[31] S. B. Field and C. Franconi, Physics and Technology of Hyperthermia, Martinus Nijhoff Publishers, Dordrecht 1987.
[32] S. U. S. Choi, Proc. ASME Int. Mech. Eng. Congr. Expo. **66**, 99 (1995).

[33] S. U. S. Choi, Z. G. Zhang, W. Yu, F. E. Lockwood, and E. A. Grulke, Appl. Phys. Lett. **79**, 2252 (2001).
[34] J. Buongiorno and W. Hu, Nanofluid Coolants for Advanced Nuclear Power Plants, Paper no. 5705, in: Proceedings of ICAPP '05, Seoul, May 15-19, 2005.
[35] N. S. Akbar and S. Nadeem, Commun. Theor. Phys. **56**, 761 (2011).
[36] N. S. Akbar, S. Nadeem, T. Hayat, and A. A. Hendi, Heat Mass Transf. **48**, 451 (2012).
[37] N. S. Akbar and S. Nadeem, Heat Transf. **41**, 10 (2012).
[38] M. Mustafa, S. Hina, T. Hayat, and A. Alsaedi, Int. J. Heat Mass Transf. **55**, 4871 (2012).
[39] N. S. Akbar, S. Nadeem, T. Hayat, and A. A. Hendi, Meccanica **47**, 1283 (2012).
[40] A. Ebaid and E. H. Aly, Comput. Math. Methods Med. **2013**, (2013), Article ID 825376, 8 pages.
[41] T. Hayat, M. Hussain, M. Awais, and S. Obaidat, Int. J. Numer. Methods Heat Fluid Flow **23**, 1155 (2013).
[42] S. Noreen, B. Ahmed, and T. Hayat, Plos one **8**, e73248 (2013).
[43] M. Mustafa, T. Hayat, and A. Alsaedi, J. Mechanics **29**, 423 (2013).
[44] N. T. Eldabe, E. M. Elghazy, and A. Ebaid, Phys. Lett. A **363**, 257 (2007).
[45] A. Ebaid, Commun. Nonlin. Sci. Numer. Simul. **15**, 1921 (2011).
[46] A. Ebaid, J. Comput. Appl. Math. **235**, 1914 (2011).
[47] A. M. Wazwaz, Int. J. Comput. Math. **88**, 3406 (2011).
[48] A. Ebaid, Z. Naturforsch. **66a**, 423 (2011).
[49] E. H. Ali, A. Ebaid, and R. Rach, Comput. Math. Appl. **63**, 1056 (2012).
[50] M. Dehghan and A. Taleei, Appl. Math. Model. **36**, 2340 (2012).